Enhancing Therapeutic Loading and Delaying Transport via Molecular Imprinting and Living/Controlled Polymerization

Asa D. Vaughan, Jeney B. Zhang, and Mark E. Byrne
Biomimetic & Biohybrid Materials, Biomedical Devices, and Drug Delivery Laboratories, Dept. of Chemical Engineering, Auburn University, Auburn, AL 36849

DOI 10.1002/aic.11949
Published online August 26, 2009 in Wiley InterScience (www.interscience.wiley.com)

This work demonstrates for the first time molecular imprinting using a ''living/controlled'' polymerization (LCP) strategy to enhance template loading/affinity and delay release in weakly crosslinked gels. Two gel systems were studied: poly(DEAEM-co-HEMA-co-PEG200DMA) gels imprinted for diclofenac sodium and poly(MAA-co-EGDMA) gels imprinted for ethyl adenine-9-acetate. Experimental evidence confirms that template diffusion coefficients within imprinted gels can be heavily influenced by template binding affinity. Recognition studies revealed significant increases in template loading/affinity with large increases in loading for LCP, and dynamic template release studies showed that imprinting via LCP extends the template release profile by twofold over that of imprinting via conventional free-radical polymerization techniques and fourfold over the control network (less Fickian and toward zero-order release with a profile coefficient of 0.70). Analysis of reaction kinetics indicated that LCP with reversible termination events increases the chemically controlled chain propagation mechanism, and that binding sites are formed during this phase of the polymerization.
 AIChE J, 56: 268–279, 2010
Keywords: molecular imprinting, controlled drug delivery, living/controlled polymerization, anti-inflammatory hydrogels, iniferter

Introduction

In the field of controlled therapeutic delivery, therapeutic release from swollen gels typically agrees with the Fickian model of release kinetics, which means that the therapeutic release rate is proportional to the therapeutic concentration gradient.[1,2]

Macromolecular memory within heteropolymer gels is a relatively new method for additional control of therapeutic diffusion within gels[2–9] and is especially useful within decreased length scales, as with controlled therapeutic delivery via thin films and coatings. Molecular imprinting techniques introduce ''macromolecular memory'' within gels and increase the tailorability of the macromolecular structure by producing gel networks with intrinsic affinity and capacity for a template molecule. The advantage of tuning copolymer network functionality is the ability to manipulate the macromolecular structure on the scale of the therapeutic, thus providing better control over the drug release rate.[2–9] Increasing the number of therapeutic molecules to polymer chains within a given gel volume is also a significant advantage and significantly increases the therapeutic payload. Recently, these techniques have demonstrated extended therapeutic release and enhanced loading within thin hydrogel films for application within ocular delivery.[2–8] Our group was the first to demonstrate enhanced loading and delayed release in hydrogels because of a diversity of monomers,[3] and the work of Alvarez-Lorenzo et al.[5] was the first to demonstrate significant dependence on the functional monomer/template ratio. A recent review of imprinting within gels highlights the immense potential and status of the field.[9]

Correspondence concerning this article should be addressed to M. E. Byrne at byrneme@eng.auburn.edu

Iniferters, which are initiator-chain transfer molecules pioneered by Otzu and Yoshida, and Matyjaszewsk,[10,11] have been used to create linear polymer chains with low polydispersities.[12–14] ''Living/controlled'' polymerization (LCP) reactions have been used to create linear polymers of uniform chain length,[15–18] specific block copolymers,[19–24] and grafted polymers on silicon surfaces.[25–30] Shorter kinetic chain lengths have been shown with ''living/controlled'' homopolymerization of methacrylic anhydride,[31] and structural evolution of networks has been studied with living polymerization.[32] Surprisingly, there is not much work in the literature on the use of living polymerization to produce and control the formation of polymer networks.

Examples of ''living/controlled'' techniques include, the use of ring opening metathesis polymerization,[33] organometallic molecules,[15,34] and atom transfer radical polymerization[15,35] (ATRP), reverse ATRP,[17,36] tellurium-mediated polymerization (TERP),[37] and nitroxide-mediated polymerization (NMP).[38] In this work, we exploit reversible addition-fragmentation chain transfer polymerization ''living'' polymerization with an iniferter that decays upon UV irradiation into more stable dithiocarbamyl (DTC) radicals, which do not actively initiate the polymerization. The termination step within ''living'' polymerization is significantly different from conventional free-radical termination events. Within ''living'' polymerization, the DTC radical reacts with the propagating chain forming a macroiniferter. The macroiniferter can decay back into a DTC radical and a propagating chain during the polymerization. Thus, LCP adds a reversible termination step to the polymerization reaction.[39] It is important to note that although there are many different types of mechanisms, virtually all the methodologies have a reversible termination step with dormant species that can be reactivated.

In this work, we are the first to use LCP techniques to prepare imprinted, weakly crosslinked networks, and the first to demonstrate enhanced template loading and extended template release profiles with imprinted gel networks formed via LCP. Our gels synthesized via LCP demonstrate very high template loading capacities when compared with literature values.[2,9]

Using living polymerization in the creation of imprinted networks to enhance or optimize template binding parameters is relatively new. The first evidence in the field to demonstrate this phenomena in highly crosslinked systems appeared in 2006 by two separate groups.[40,41] Our group demonstrated that LCP techniques applied to molecular imprinting resulted in enhanced template loading in highly crosslinked ethyl adenine-9-acetate-imprinted poly(methacrylic acid-*co*-ethylene glycol dimethacrylate) networks.[40,42] The LCP with a reversible termination reaction can provide much more control over the network structure. It increased the potential for the growing polymer network and template binding complexes to reach a global energy minimum and led to further memorization of the chain conformation. Compared to conventional techniques, LCP resulted in a 63% increase in the number of binding sites at approximately equivalent average binding affinity while retaining selectivity for the template. This was hypothesized to be attributed to a decrease in kinetic chain length and/or a more narrow dispersity of kinetic chains, which leads to increased structural homogeneity with more stability and integrity of more appropriately sized binding sites.

Yei and coworkers[41] used nitroxide-mediated living polymerization to produce highly crosslinked imprinted polymers via a sacrificial covalent bond. Once hydrolyzed, the imprinted networks prepared via living polymerization displayed higher selective cholesterol binding. The sacrificial covalent bond was crucial to produce a successfully imprinted polymer because of a high temperature of reaction, which was needed for the nitroxide-mediated living polymerization.

It is also important to note that living polymerization has been used successfully to surface graft imprinted films.[43,44] Although these methods exploit LCP techniques, the primary concern is grafting or attaching the polymer layers or the polymer to a composite material and not on the enhancement of the template binding parameters. Thus, it should be distinctly understood that the transition toward enhanced binding parameters is very significant and is a new direction in the field.

Another significant aspect of this work is the release of the anti-inflammatory therapeutic, diclofenac sodium, from thin film hydrogels. The hydrogels in this work could be an important material to produce extended release anti-inflammatory releasing lenses, which have been produced for timolol,[5,7] ketotifen fumarate,[2,3] and hyaluronic acid.[8]

Materials and Methods

The monomers, methacrylic acid (MAA) and ethylene glycol dimethacrylate (EGDMA), had inhibitors removed via inhibitor removal packing sieves or vacuum distillation before polymerization. The monomers (diethylaminoethyl methacrylate (DEAEM) and 2-hydroxyethyl methacrylate (HEMA)), the initiator (azo-bis(isobutyronitrile) (AIBN)), template molecules (ethyl adenine-9-acetate (EA9A) and diclofenac sodium), and iniferter (tetraethylthiuram disulfide (TED)) were used as received. Monomers, inhibitor removal packing sieves, initiator, iniferter, and template were purchased from Aldrich (Milwaukee, WI). Polyethylene glycol 200 dimethacrylate (PEG200DMA) was purchased from Polysciences (Warrington, PA). HPLC grade solvents, acetonitrile and methanol, were used as received from Fisher Scientific (Pittsburgh, PA). The polymer wash solvent (to remove template and unreacted monomer) was acetonitrile/methanol at a 4:1 volume ratio for the EA9A-imprinted networks or deionized (DI) water for the diclofenac sodium-imprinted networks.

Synthesis of poly(MAA-co-EGDMA) recognitive gels

A solution to produce a 5% crosslinked EA9A-imprinted poly(MAA-*co*-EGDMA) gel was made with 0.187 mL of EGDMA (0.993 mmol), 1.6 mL of MAA (18.86 mmol), 18.55 mg of AIBN (0.113 mmol), and 84.06 mg of EA9A (0.380 mmol). Solutions were placed in a sonicator for several minutes until all solids were dissolved. Control gel solutions were made exactly in the same manner except no EA9A template was added. A poly(MAA-*co*-EGDMA) recognitive gel prepared via LCP was made by addition of 3.89 mg of TED iniferter (0.013 mmol) to the solution mixture. The molar ratio of initiator divided by iniferter was 8.61. The temperature of polymerization was carefully controlled (14°C ± 1°C)

throughout the exothermic reaction, and the UV free-radical polymerization was conducted using a mercury halide source with a light intensity of 52.5 mW/cm^2, calibrated by a photometer. Temperatures lower than 14°C resulted in freezing of the prepolymerization mixture. Oxygen, which is a radical scavenger, was removed by purging the polymerization solution with nitrogen for a period of 15 min. The polymerization was carried out via UV-free radical polymerization in a Q-100 differential photo calorimeter (DPC) from TA Instruments (New Castle, Delaware) resulting in a polymer disk with a diameter of 3 mm and a thickness of 1 mm. The DPC allowed strict temperature control within ±1°C.

All poly(MAA-*co*-EGDMA) gels were washed in a modified Soxhlet extraction device to ensure that the disks were immersed in solvent at all times. The wash was stopped after the template was no longer detected in the effluent. The discs were allowed to dry under laboratory conditions at a temperature of ~20°C for 24 h and then transferred to a vacuum oven (27 in Hg, 33–34°C) for 24 h until the disc weight change was less than 0.1 wt %.

Synthesis of poly(DEAEM-co-HEMA-co-PEG200DMA) recognitive gels

Diclofenac sodium-imprinted poly(DEAEM-*co*-HEMA-*co*-PEG200DMA) gels with a 5% crosslinking percentage were made with 0.336 mL of DEAEM (1.673 mmol), 3.659 mL of HEMA (30.118 mmol), 0.538 mL of PEG200DMA (1.673 mmol), 20 mg of AIBN (0.121 mmol), and 150 mg of diclofenac sodium (0.352 mmol). The solutions were mixed and sonicated until all solids were dissolved, and control gel solutions were prepared without template. The poly(DEAEM-*co*-HEMA-*co*-PEG200DMA) recognitive gel prepared via LCP was synthesized with 4.20 mg of TED (0.014 mmol) and 40 mg of AIBN (0.242 mmol). Solutions were transferred to an MBraun Labmaster 130 1500/1000 Glovebox (Stratham, NH), which provided an inert (nitrogen) atmosphere for free-radical UV photopolymerization. Then monomer solutions were pipetted between two 6" × 6" glass plates coated with trichloromethylsilane (to prevent strong adherence of the polymer matrix to the glass) and separated by 0.25 mm Teflon spacers. The solutions were left uncapped and open to the nitrogen atmosphere until the O_2 levels inside reached negligible levels (<1 ppm). The polymerization reaction was carried out for 8 min for the poly(DEAEM-*co*-HEMA-*co*-PEG200DMA) control and recognitive gels, whereas for the LCP prepared polymers the reaction time was 24 min. Separate DPC studies revealed exact reaction times. The intensity of light from a UV Flood Curing System (Torrington, CT) was 40 mW/cm^2 at a voltage of 325 V, and the temperature within the glovebox was held constant at 25°C.

After polymerization, the glass plates were soaked in DI water and the polymers were quickly peeled off the plates and cut into circular discs using a size 10 cork borer (13.5 mm). The gels were washed in a well-mixed 2 L container of DI water for 7 days with a constant 5 mL per minute flowrate of DI water. Absence of detectable drug released from the polymer gel was verified by removing random gels, placing them in fresh DI water with adequate mixing, and sampling the supernatant via spectroscopic monitoring. The discs were allowed to dry under laboratory conditions at a temperature of 20°C for 24 h and then transferred to a vacuum oven (27 in Hg, 33–34°C) for 24 h until the disc weight change was less than 0.1 wt %.

Template recognition studies

Binding studies were conducted in acetonitrile and DI water for the poly(MAA-*co*-EGDMA) and the poly (DEAEM-*co*-HEMA-*co*-PEG200DMA) gels, respectively. For the poly(DEAEM-*co*-HEMA-*co*-PEG200DMA) gel experiments, a stock solution of 1 mg/mL of diclofenac sodium was prepared and diluted to five concentrations (0.05, 0.10, 0.15, 0.20, and 0.25 mg/mL). Initial absorbances of each concentration were measured using a Synergy UV–vis spectrophotometer (BioTek Instruments, Winooski, VT) at 276 nm, the wavelength of maximum absorption. After the initial absorbance was taken, a dry, washed poly(DEAEM-*co*-HEMA-*co*-PEG200DMA) polymer disk was inserted in each vial and the vials were gently mixed until equilibrium. Separate dynamic studies were performed to assure equilibrium conditions were reached. After equilibrium was reached over a 7-day period, the solutions were vortexed for 10 s, and the equilibrium concentrations were measured. A mass balance was used to determine the bound amount of drug within the polymer gel. All gels were analyzed in triplicate, and all binding values are based upon the dry weight of the gel.

Similar methods were used with EA9A-imprinted gels except that binding studies reached equilibrium in 24 h, different template concentrations were used, and acetonitrile was the rebinding solvent. The wavelength of absorbance for EA9A was 265 nm.

The Freundlich isotherm (Eq. 1) was used to determine binding parameters because it gave the best fit to the experimental data.

$$Q = k_f C_e^n \tag{1}$$

The amount bound by the recognitive polymer is Q, C_e is the equilibrium concentration, and k_f is the affinity. The maximum affinity (K_{max}) and minimum affinity (K_{min}) can be calculated from the maximum and minimum equilibrium concentrations ($C_{e\,max}$ and $C_{e\,min}$) as described in Eq. 2.

$$K_{min} = \frac{1}{C_{e\,max}} \quad \text{and} \quad K_{max} = \frac{1}{C_{e\,min}} \tag{2}$$

The number of binding sites ($N_{K_1\text{-}K_2}$) between affinities K_1 and K_2 and the average affinity ($\overline{K}_{K_1-K_2}$), which is between K_{min} and K_{max}, were calculated using Eqs. 3 and 4.

$$N_{K_1-K_2} = k_f(1-n^2)(K_1^{-n} - K_2^{-n}) \tag{3}$$

$$\overline{K}_{K_1-K_2} = \left(\frac{n}{n-1}\right)\left(\frac{K_1^{1-n} - K_2^{1-n}}{K_1^{-n} - K_2^{-n}}\right) \tag{4}$$

Dynamic template release studies and diffusion coefficient determination

After binding studies, template loaded gels, loaded at a template concentration of 0.25 mg/mL, were placed in a Sotax Dissolution Apparatus (Horsham, PA) with 1000 mL

of artificial lacrimal solution. The artificial lacrimal solution was prepared with 6.78 g/L NaCl, 2.18 g/L $NaHCO_3$, 1.38 g/L KCl, and 0.084 g/L $CaCl_2 \cdot 2H_2O$, and the pH was 8.0.[45] The solution was stirred at a constant rate of 75 rpm by paddles and kept at a constant temperature of 37°C. At various time points, the absorbance of the solution was measured using a Synergy UV–vis spectrophotometer (BioTek Instruments, Winooski, VT) at 276 nm until the concentration did not change more than 1%.

Fractional template release profiles were calculated for the diclofenac recognitive and control gels by taking the amount of template released at specific times, M_t, divided by the maximum amount of diclofenac released during the experiment, M_∞. The fractional template release profile, M_t/M_∞ vs. time, was determined for each gel. Template diffusion coefficients were calculated using Fick's law, which describes one-dimensional planar solute release from gels.[46] For polymer geometries with aspect ratios (exposed surface length/thickness) greater than 10, edge effects can be ignored and the problem approached as a one-dimensional process.[46] Solution of Fick's law for short times of diffusion is given by Eq. 5,

$$\frac{M_t}{M_\infty} = 4\left[\frac{Dt}{\pi L^2}\right]^{\frac{1}{2}} \tag{5}$$

where M_t is the mass of template released at time t, M_∞ is the mass of template released at infinite time, D is the diffusion coefficient independent of position and concentration, and L is the thickness of the polymer. For each polymer network, the fractional release of template (M_t/M_∞) vs. ($t^{0.5}/L$) was plotted and the diffusion coefficient was calculated from the slope. The exponent, n, was also calculated using the empirical relationship $M_t/M_\infty = kt^n$. An exponent value of 0.5 from a disk indicates Fickian diffusion, and a value of 1 indicates zero order or constant release.

For the EA9A-imprinted poly(MAA-*co*-EGDMA)gels, template loaded gels were placed in 25 mL of acetonitrile, and the solutions were mixed using an Ocelot oscillator (Boekel Scientific, Feasterville, PA). Separate studies were conducted to assure an infinite sink, and the fluid was changed every 8 h for the first 36 h and thereafter every 24 h. At every fluid change, a 200 μL aliquot was taken and the EA9A concentration was measured via absorbance at a wavelength of 265 nm.

Gel swelling and structural studies

The equilibrium weight swelling ratio was obtained by taking the ratio of the swollen weight to the dry weight. The equilibrium volume swelling ratio, Q, was calculated as follows:

$$Q = \frac{1}{\upsilon_{2,S}} = \frac{V_{2,S}}{V_{2,d}} \tag{6}$$

where $V_{2,\,S}$ is the swollen gel volume at equilibrium, $V_{2,\,d}$ is the volume of the dry polymer, and $\upsilon_{2,s}$ is the polymer volume fraction in the swollen state. The dry and swollen gels were weighed in air and heptane, a nonsolvent, using a microbalance (Sartorius). The volume of the gel in the swollen or dry state was obtained by using Archimedes buoyancy principle with heptane (density of 0.684 g/mL at a temperature of 25°C). Gels in the relaxed state were weighed immediately after polymerization without exposure to solvent.

Dynamic swelling studies were performed by placing dry polymer disks in solvent and weighing at various time intervals by removing the gels from the swelling media and blotting with absorbent, lint-free tissue to remove excess surface solvent.

Hydrogel structural analysis was obtained by swelling and tensile experimental studies and by using the theory of rubber elasticity. Static experiments were performed in the equilibrium swollen state. Samples of each gel (1 mm × 5 mm × 15 mm strips) were removed from the solvent and analyzed with a RSA III Dynamic Mechanical Analyzer (DMA), (TA Instruments, New Castle, DE) to obtain stress vs. strain.

The following equation[47,48] takes into account the polymer swollen until equilibrium with the solvent, but not prepared in solvent.

$$\tau = RT\left(\frac{1}{\bar{v}\overline{M}_c}\right)\left(1 - \frac{2\overline{M}_c}{M_n}\right)\left(\alpha - \frac{1}{\alpha^2}\right)\upsilon_{2,s}^{1/3} \tag{7}$$

where τ is the normal stress applied, α is the deformation of the network structure by elongation which is equivalent to the stretched length over initial length ($\alpha = L/L_o$), $\bar{v}$ is the specific volume of the polymer in the relaxed state, M_n is the number-average molecular weight, and $\overline{M}_c$ is the average molecular weight between crosslinks, R is the universal gas constant, and T is the temperature. Because $\overline{M}_c \ll M_n$, Eq. 7 simplifies further and the stress/strain data obtained from DMA were plotted with the deformation term on the y-axis and tension, τ, on the x-axis to obtain the slope, from which the average molecular weight between crosslinks, $\overline{M}_c$, was calculated. To determine the mesh size, ξ, of the polymer network, the relationship of ξ to $\overline{M}_c$ was determined from the work of Peppas and coworkers,[1,49]

$$\xi = Q^{1/3}\left(2C_n\left(\frac{\overline{M}_c}{M_r}\right)\right)^{1/2} l \tag{8}$$

where Q is the equilibrium volume swelling ratio, C_n is the Flory characteristic ratio for the polymer (obtained from a molar average of the homopolymers), and M_r is the effective molecular weight of the repeating unit (determined by a weighted average of the copolymer composition). The C_n values used in this analysis were 14 for polymethacrylic acid, 3.8 for polyethylene glycol dimethacrylate, and 11 for poly(DEAEM-*co*-HEMA-*co*-PEG200DMA), a typical average value of the characteristic ratio.[50–53] The carbon–carbon bond length of the polymer backbone, which is equal to 1.54 Å, is represented by length, l.

Kinetic analysis of polymerization reaction

A dark reaction was used to determine the kinetic reaction profile for the poly(MAA-*co*-EGDMA) gels.[54,55] For each polymerization reaction, the UV light was shut off at a specific time point during the reaction. The rate of polymerization was calculated via reaction analysis using the heat flow

vs. time results from the DPC, average molecular weight of the polymerization solution, and the theoretical heat of reaction. Fractional double bond conversion was determined by dividing the experimental heat of reaction by the theoretical heat of reaction. The experimental heat of reaction was determined by the area under the heat flow vs. time curve from the DPC. The termination and propagation constants, k_t and k_p, were calculated from Eqs. 9 and 10, and the derivation of these equations can be found in Odian or Flory.[48,56]

$$\frac{k_p}{k_t^{\frac{1}{2}}} = \frac{Rp}{[M](fI_o\varepsilon[I])^{\frac{1}{2}}} \tag{9}$$

where [M] represents the monomer concentration, the initiator efficiency is f, I_o is the light intensity, ε is the extinction coefficient, and [I] is the initiator concentration. The unsteady state equation used to decouple the propagation constant and the termination constant is shown later,

$$k_t^{\frac{1}{2}} = \frac{\frac{k_p}{k_t^{\frac{1}{2}}}}{2(t_1 - t_0)}\left[\frac{[M]_{t=t_1}}{Rp_{t=t_1}} - \frac{[M]_{t=t_o}}{Rp_{t=t_o}}\right] \tag{10}$$

where $t_1$and t_0 are the final and initial times, $[M]_{t=t1}$ and $[M]_{t=t0}$ are the corresponding monomer concentrations, and $Rp_{t=t1}$ and $Rp_{t=t0}$ are the rate of polymerization at the final and initial times, respectively.

Results and Discussion

Template recognition

Template binding results for poly(MAA-*co*-EGDMA) gels are presented in Figure 1. The most dramatic results are seen comparing template loading capacity. As demonstrated by the equilibrium binding isotherm, the poly(MAA-*co*-EGDMA) recognitive gel had a 42% increase in template binding capacity over that of the control network. The template loading capacity for the poly(MAA-*co*-EGDMA) control gel and recognitive gel was (1.40 ± 0.30 and 2.00 ± 0.20) $\times 10^{-2}$ mmol/g, respectively. The increase in capacity results from the macromolecular memory produced by the imprinting process. The concept of macromolecular recognition within gels manifests itself from two major synergistic effects, (i) memory cavities produced from multiple flexible chains, which primarily stabilize the chemistry in a crosslinked network, and (ii) chemical groups oriented to form multiple complexation points with the template. Macromolecular memory and the imprinting effect demonstrated in weakly crosslinked gels are significant because most imprinted systems to date are highly crosslinked. Only recently has the molecular imprinting technique been demonstrated within flexible networks.[2–8]

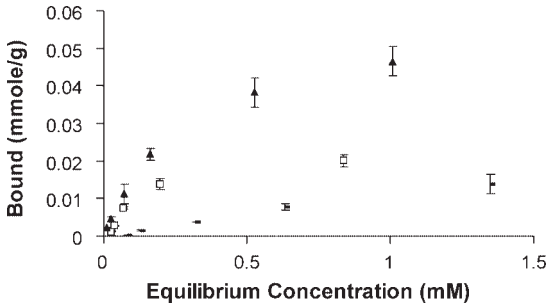

Figure 1. Poly(MAA-*co*-EGDMA) gel binding isotherms for ethyl adenine-9-acetate in acetonitrile.

Data points represent the poly(MAA-*co*-EGDMA) control gel(—), the poly(MAA-*co*-EGDMA) recognitive gel (□), and the poly(MAA-*co*-EGDMA) recognitive gel prepared via "living/controlled" polymerization (▲). The poly(-MAA-*co*-EGDMA) recognitive gel prepared via "living/controlled" polymerization has a loading capacity 90% higher than the poly(MAA-*co*-EGDMA) recognitive gel capacity and a 171% increase over the control network. Error bars represent the standard error with $n = 4$.

The poly(MAA-*co*-EGDMA) recognitive gel prepared via LCP had a 90% increase in template binding capacity ($3.80 \pm 0.40 \times 10^{-2}$ mmol/g) compared with the recognitive gel prepared via conventional free-radical polymerization and a 171% increase in template binding capacity over the control (Figure 1). The increase in template binding capacity for the gel formed via "living" polymerization indicates enhanced macromolecular memory for the template above typical free-radical polymerization methods. For weakly crosslinked systems, this has not been demonstrated earlier in the literature. Recently, our group was the first to publish evidence of enhanced binding parameters for highly crosslinked systems.[40,42]

The templating or imprinting effect is also evident in the calculated template binding affinities. Binding affinities calculated by Freundlich isotherm analysis for the poly(MAA-*co*-EGDMA) control gel, recognitive gel, and recognitive gel prepared via LCP were 1.93 ± 0.10, 2.45 ± 0.13, and 2.21 ± 0.11 mM^{-1}, respectively. The recognitive gel and the recognitive gel prepared via LCP had similar average template affinities; however, both recognitive gels had higher average affinities than the control network. The increased template binding affinity is a direct result of imprinting. All the binding parameters for the weakly crosslinked poly(MAA-*co*-EGDMA) networks are presented in Table 1.

Table 1. Poly(MAA-*co*-EGDMA) and Poly(DEAEM-*co*-HEMA-*co*-PEG200DMA) Gel Template Binding Affinity and Capacity Comparing Conventional and Living/Controlled Polymerization

Gel Type	Template	K_a (mM^{-1})	Capacity (mmol/g)
Poly(DEAEM-*co*-HEMA-*co*-PEG200DMA) recognitive gel	Diclofenac	15.05 ± 0.82	$2.30 \pm 0.20 \times 10^{-2}$
Poly(DEAEM-*co*-HEMA-*co*-PEG200DMA) recognitive gel prepared via "living/controlled" polymerization	Diclofenac	14.57 ± 0.73	$3.54 \pm 0.16 \times 10^{-2}$
Poly(DEAEM-*co*-HEMA-*co*-PEG200DMA) control gel	None	9.91 ± 0.49	$0.96 \pm 0.12 \times 10^{-2}$
Poly(MAA-*co*-EGDMA) recognitive gel	EA9A	2.45 ± 0.13	$2.00 \pm 0.20 \times 10^{-2}$
Poly(MAA-*co*-EGDMA) recognitive gel prepared via "living/controlled" polymerization	EA9A	2.21 ± 0.11	$3.80 \pm 0.40 \times 10^{-2}$
Poly(MAA-*co*-EGDMA) control gel	None	1.93 ± 0.10	$1.40 \pm 0.30 \times 10^{-2}$

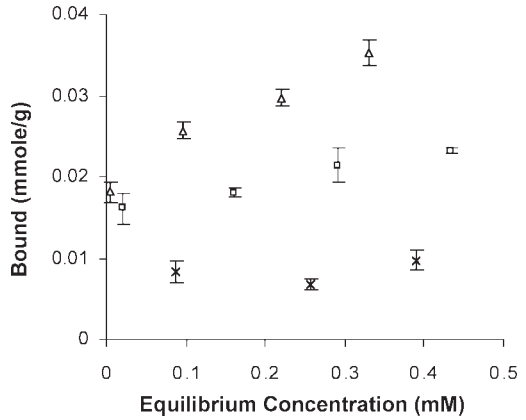

Figure 2. Poly(DEAEM-*co*-HEMA-*co*-PEG200DMA) gel binding isotherms for diclofenac sodium in water.

Poly(DEAEM-*co*-HEMA-*co*-PEG200DMA) recognitive gel via "living/controlled" polymerization techniques (Δ) shows a 54% increase in loading capacity over that of poly (DEAEM-*co*-HEMA-*co*-PEG200DMA) recognitive gel (□). Both recognitive gels bound more diclofenac sodium compared with the control gel (x), and the recognitive gel had a 140% increase in template loading over that of the control network, the recognitive gel prepared via "living/controlled" polymerization had a 269% increase over that of the control gel. Error bars represent the standard error with $n = 3$.

These results have also been confirmed in another polymer gel system using a different template. Diclofenac sodium binding results for the poly(DEAEM-*co*-HEMA-*co*-PEG200DMA) control gel, recognitive gel, and the recognitive gel prepared via LCP are presented in Figure 2. The poly(DEAEM-*co*-HEMA-*co*-PEG200DMA) recognitive gel had a 140% increase in template loading over that of the control network, with loading capacities of (0.96 ± 0.12 and 2.30 ± 0.20) $\times 10^{-2}$ mmol/g, respectively. The recognitive gel prepared via LCP had a 54% increase in template loading capacity (3.54 ± 0.16) $\times 10^{-2}$ mmol/g) over that of the recognitive gel and a 269% increase over that of the control gel. Both recognitive gels had ~1.5 times higher template binding affinity than the control gel, which had a template binding affinity of 9.91 ± 0.49 mM^{-1}. All binding parameters for the diclofenac-imprinted poly(DEAEM-*co*-HEMA-*co*-PEG200DMA) gels are presented in Table 1.

Although these networks demonstrate similar trends and numerical values in capacity and percent increase in capacity, the poly(MAA-*co*-EGDMA) gels have significantly smaller binding affinities compared with the poly(DEAEM-*co*-HEMA-*co*-PEG200DMA) gels. This is due to differences in the noncovalent template–polymer binding strength and the network structure itself, and it is reflected in comparison of the binding isotherms with poly(DEAEM-*co*-HEMA-*co*-PEG200DMA) gels exhibiting higher binding at lower concentrations.

The poly(MAA-*co*-EGDMA) gels primarily exploit hydrogen bonding in recognition of EA9A in acetonitrile. The poly(DEAEM-*co*-HEMA-*co*-PEG200DMA) gel uses ionic bonding in conjunction with hydrogen bonding to recognize diclofenac sodium in water. Ionic bonds are the strongest noncovalent bonds with bond strengths of 5–35 kcal/mol, approaching a third of covalent bond strength, and are 20–30 times stronger than hydrogen bonds.[57,58] Stronger noncovalent bonds are manifested in higher binding affinities via macromolecular memory for the template.

It is important to note that the rebinding solvents were different with acetonitrile and water being used for the poly (MAA-*co*-EGDMA) gel and poly(DEAEM-*co*-HEMA-*co*-PEG200DMA) gel studies, respectively. A polar, protic solvent has a permanent dipole moment and can form hydrogen bonds. A polar, aprotic solvent has a permanent dipole moment, but cannot form hydrogen bonds. Water is a polar, protic solvent and acetonitrile is a polar, aprotic solvent with dielectric constants of 80.4 and 37.5 at a temperature of 25°C, respectively. Thus, each system exploits a different, yet effective, intended noncovalent template polymer binding event by careful selection of solvent. If hydrogen bonding was the primary bonding force for the template polymer in an aqueous environment, water would compete and weaken template–polymer interactions.

Reaction double bond conversion

Structural differences can be due to differences in monomer conversion and crosslinking monomer. Poly(DEAEM-*co*-HEMA-*co*-PEG200DMA) imprinted gels were synthesized using a crosslinker with ~4.5 more ethylene glycol groups than the poly(MAA-*co*-EGDMA) gels. This longer crosslinker increased interchain network flexibility and has been shown to lead to decreases in binding affinity and capacity.[59]

To ensure the enhanced loading from the poly(MAA-*co*-EGDMA) and poly(DEAEM-*co*-HEMA-*co*-PEG200DMA) gels prepared via LCP was not due to differences in monomer conversion, reaction analysis was performed to determine double bond conversion. The double bond conversion calculated via reaction analysis for the poly(MAA-*co*-EGDMA) recognitive gel and the recognitive gel prepared via LCP was 56% ± 3.2% and 59% ± 3.5%, respectively. There were also no statistical differences between the poly (DEAEM-*co*-HEMA-*co*-PEG200DMA) recognitive gel and the gel prepared via LCP, which had double bond conversions of 80% ± 5.1% and 83% ± 4.7%, respectively. Higher conversions with longer crosslinking monomers have been shown to be a result of increased flexibility resulting in lower amounts of pendant double bonds,[42] thus longer crosslinking monomer chains have a higher reactivity. Pendant double bonds are sterically hindered by the surrounding polymer network and cannot react with surrounding radical chains.

These results conclusively rule out increases in template binding capacity because of increased double bond conversion. Significant differences in reacted double bonds may indicate differences in polymer structure, which could alter the polymer binding characteristics. Because conversion is held constant, structural changes induced via the "living/controlled" templating polymerization mechanism can be studied.

To determine whether the increase in template loading via "living" polymerization techniques was due to a incorporation of more functional monomer within the network, a poly (DEAEM-*co*-HEMA-*co*-PEG200DMA) control gel was prepared using LCP. It is important to note that the control gel

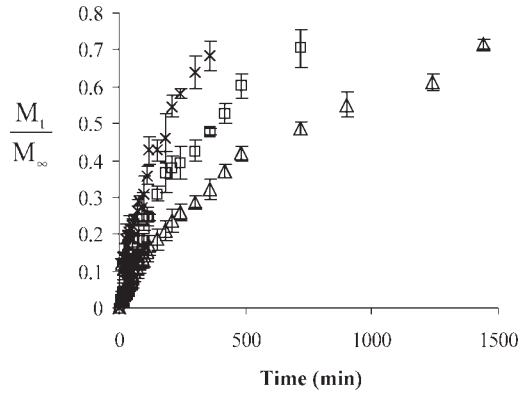

Figure 3. Fractional release of diclofenac sodium template for poly(DEAEM-*co*-HEMA-*co*-PEG200DMA) gels.

The recognitive gel prepared via "living/controlled" polymerization (Δ) had extended release in water when compared with the recognitive gel (□) and the control gel (x). The error bars represent the standard error with $n = 3$.

was synthesized in the exact same manner as the recognitive gel excluding the template molecule. A control gel formed via LCP having a higher binding capacity than the control gel made with standard free-radical polymerization would indicate an increase in template nonspecific binding. Thus, the enhanced loading results could be explained by a greater percentage of functional monomer incorporated in the network (i.e., LCP techniques affected the reactivity ratios). However, the equilibrium template binding isotherm for the poly(DEAEM-*co*-HEMA-*co*-PEG200DMA) control gel prepared via LCP was a statistical match to the poly(DEAEM-*co*-HEMA-*co*-PEG200DMA) control gel isotherm. Similar binding parameters indicate that LCP does not affect the nonspecific binding or the amount of functional monomer incorporated within the gel.

Template transport and network structure

Dynamic fractional and cumulative template release studies for the diclofenac sodium-imprinted poly(DEAEM-*co*-HEMA-*co*-PEG200DMA) gels are shown in Figures 3 and 4, respectively. The recognitive gel showed a twofold extension in template release time compared with the control gel (i.e., the recognitive gel released 70% of template over 700 min compared with 300 min for the control). For the gel formed via LCP, 70% template was released over a time period of 1400 min. Imprinting via "living" polymerization extends or delays the template release profile by twofold over that of imprinting via conventional free-radical polymerization techniques and fourfold over that of the control network.

Template effective diffusion coefficients were determined from the release data and quantitatively highlight these differences. The template diffusion coefficients for the control gel, recognitive gel, and the recognitive gel prepared via LCP were $6.37 \pm 1.02 \times 10^{-9}$ cm^2/s, $3.20 \pm 0.48 \times 10^{-9}$ cm^2/s, and $1.49 \pm 0.33 \times 10^{-9}$ cm^2/s, respectively. The control gel had a two- and fourfold higher diffusion coefficient than the recognitive gel and recognitive gel prepared via LCP, respectively.

The release profiles of the recognitive gel and recognitive gel prepared via LCP are less Fickian and moving toward zero-order release with profile coefficients of 0.68 and 0.70, respectively. The control gel conforms very well to a Fickian release profile with $n = 0.48$. Thus, molecular imprinting shifted the release profiles toward zero-order template release, or constant release that is not dependent upon time or template concentration. Exploiting LCP methods contributes further control upon the template release characteristics of the hydrogel. Our research group has recently demonstrated that slower release profiles for imprinted gels is due to the intrinsic template binding characteristics of the polymer network, and may be best explained by the "tumbling hypothesis."[2] The hypothesis states that as the template molecule diffuses through the network it binds and unbinds a number of times to multiple binding sites as it diffuses through the network.

The cumulative release profiles (Figure 4) highlight the total amount of diclofenac template released by each poly (DEAEM-*co*-HEMA-*co*-PEG200DMA) gel. The recognitive gel releases 179% more template compared with the control network over a period of 7 days, with 1.34 ± 0.04 mg and 0.48 ± 0.01 mg of diclofenac sodium released. This indicates that macromolecular memory increases the template loading capacity and confirms the increase in template binding shown in the binding analysis. The recognitive gel prepared via LCP released 1.87 ± 0.06 mg or 34% more drug over a 7-day period in a more controlled manner than the recognitive gel prepared by conventional polymerization. This is also reflected in the binding analysis, with these gels binding the most template of all gels studied.

To further understand and confirm these results, structural analysis was performed starting with dynamic swelling experiments. Dynamic volume swelling studies for the diclofenac sodium-imprinted poly(DEAEM-*co*-HEMA-*co*-PEG200DMA) gels are presented in Figure 5. The recognitive and control gels had identical profiles indicating that the networks are structurally and compositionally very similar.

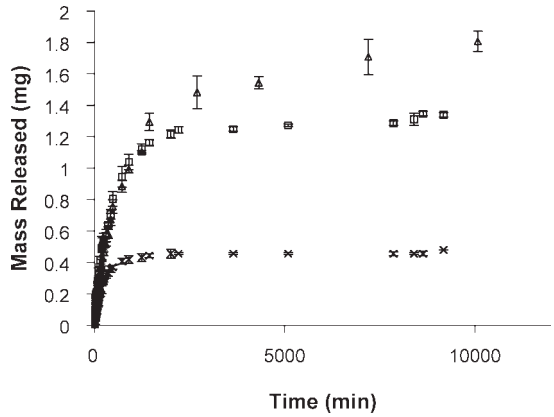

Figure 4. Cumulative mass released of diclofenac sodium template for poly(DEAEM-*co*-HEMA-*co*-PEG200DMA) gels.

The recognitive gel prepared via "living/controlled" polymerization (Δ) released a higher amount of diclofenac sodium in water when compared with the recognitive gel (□) and the control gel (x). The error bars represent the standard error with $n = 3$.

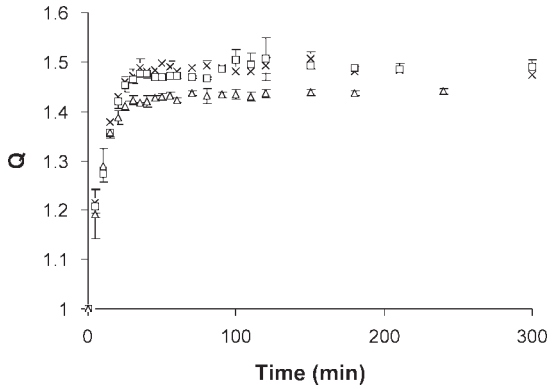

Figure 5. Dynamic volume swelling studies for poly (DEAEM-*co*-HEMA-*co*-PEG200DMA) gels.

The recognitive gel (□) and the control gel (x) had similar swelling characteristics in the aqueous solution of diclofenac sodium (concentration 2 mg/mL). The recognitive gel prepared via "living/controlled" polymerization (Δ) had a lower equilibrium volume swelling value and more polymer volume fraction in the swollen state, which indicates differences in macromolecular structure. The error bars represent the standard error with $n = 3$.

The dynamic swelling profile of the recognitive gel prepared via LCP is similar, but the equilibrium value is lower than both the poly(DEAEM-*co*-HEMA-*co*-PEG200DMA) control and recognitive gel indicating that the gel swells to a lesser extent and the polymer volume fraction in the swollen state is higher.

Mesh size calculations confirm these results. At equivalent double bond conversions, diclofenac-imprinted poly (DEAEM-*co*-HEMA-*co*-PEG200DMA) recognitive gels prepared with conventional polymerization and LCP methods had average mesh sizes of 30.3 ± 1.7 and 19.7 ± 2.1 Å, respectively. LCP created smaller mesh sizes, which may originate from smaller and more monodisperse kinetic chain lengths within the copolymer network, which contributes to the overall homogeneity of the network structure. LCP techniques have shown to produce shorter kinetic chain lengths and low polydispersities in linear polymer networks.[15,17,36]

Mesh sizes were also calculated for the poly(MAA-*co*-EGDMA) networks. The mesh sizes were 4.13 ± 0.20 and 4.13 ± 0.30 Å in acetonitrile for the recognitive gel and the recognitive gel prepared via LCP, respectively. The relatively small mesh size suggests that these gels are in a collapsed state. Mesh sizes for similar poly(MAA-*co*-PEGDMA) gel networks have been presented within literature ranging from 3.4–23.8 Å.[60,61] Crosslinked polymer gels in a collapsed state would have a high Flory-Huggins polymer–solvent interaction parameter with the solvent ($\chi_1 > 0$), which decreases the equilibrium swelling ratio and decreases mesh size.[47] The Flory interaction parameter is a unitless representation of the enthalpy of mixing, which relates to the thermodynamic relationships between the crosslinked polymer chains in contact with a solvent. The MAA chains prefer to associate with themselves resulting in a collapsed gel rather than being in a fully extended solvated state. It is important to note that these gels are made without solvent.

Similar mesh sizes for the poly(MAA-*co*-EGDMA) recognitive gels confirm the network structure being very similar regardless of the nature of the polymerization reaction. However, the template binding results indicate more effective binding sites with a 90% increase in capacity for the recognitive gel prepared via LCP. This disparity is probably due to the network being in a collapsed state, with memory sites able to bind the template.

Template diffusion through an imprinted polymer network can be influenced by three main variables, average mesh size, template size, and template–polymer chain interactions (i.e., the imprinting effect). Manipulation of one or more of these variables can alter the template diffusion coefficient. An increase in polymer mesh size holding template size and template–polymer chain interactions constant would correspond to an increase in template diffusion. An increase in template size holding mesh size and template–polymer chain interactions constant would correspond to a decrease in the template diffusion coefficient. An increase in template–polymer chain interactions holding template size and mesh size constant would correspond to a decrease in the template diffusion coefficient. Table 2 presents data that influence template diffusion, such as template binding affinity, template hydrodynamic radius, network average mesh size, as well as the template diffusion coefficient for each gel system.

A few trends and important points are evident making comparisons within the table. Considering the poly(DEAEM-*co*-HEMA-*co*-PEG200DMA) gels, living polymerization

Table 2. Template Diffusion Parameters of Poly(MAA-*co*-EGDMA) and Poly(DEAEM-*co*-HEMA-*co*-PEG200DMA) Imprinted Gels

Gel Type	Template	K_a (mM^{-1})	Template Molecular Weight	Template Hydrodynamic Radius (Å)	Mesh Size (Å)	Mesh Size/Template Hydrodynamic Radius Ratio	Effective Diffusion Coefficient (cm^2/s) × 10^9
Poly(DEAEM-*co*-HEMA-*co*-PEG200DMA) recognitive gel	Dicolfenac	15.05 ± 0.82	318.14	4.3	30.3 ± 1.7	7.05	3.20 ± 0.48
Poly(DEAEM-*co*-HEMA-*co*-PEG200DMA) recognitive gel prepared via "living/controlled" polymerization	Dicolfenac	14.57 ± 0.73	318.14	4.3	19.7 ± 2.1	4.58	1.49 ± 0.33
Poly(MAA-*co*-EGDMA) recognitive gel	EA9A	2.45 ± 0.13	221.22	4.5	4.13 ± 0.20	0.92	7.15 ± 0.13
Poly(MAA-*co*-EGDMA) recognitive gel prepared via "living/controlled" polymerization	EA9A	2.21 ± 0.11	221.22	4.5	4.13 ± 0.30	0.92	7.26 ± 0.15

decreases the mesh size by a factor of 1.5, which leads to more delayed release and a reduction in the template diffusion coefficient. Because the poly(MAA-*co*-EGDMA) gels are in a collapsed state, differences in mesh size are not apparent. However, in both systems, as previously described, imprinted gels prepared via living polymerization increase the template capacity at relatively similar affinities. However, it is not apparent if the delayed template transport is due to the imprinting effect.

Delayed release from an imprinted gel can result from increased template affinity and/or an increase in the number of binding sites. For example, with the number of binding sites constant, an increased affinity can lead to delayed release. Increasing the number of binding sites with the same affinity and can also lead to delayed release. This forms the basis for our group's recent "tumbling hypothesis" describing template tumbling from binding site to site diffusing out of the gel.[2] Template binding analysis showed a 54% increase of the loading capacity for the poly(DEAEM-*co*-HEMA-*co*-PEG200DMA) recognitive gel prepared via LCP over that of the recognitive gel. This would mean there are a little over 1.5 times as many sites within the same volume of polymer network (i.e., the volume of the gels was consistent, and the polymer volume fraction in the swollen state was 0.70 and 0.67), and the template molecule may bind and unbind 1.5 times as many times to sites, thus extending the dynamic release profile.

Comparing conventionally prepared gels for both systems, the diffusion coefficient for the poly(MAA-*co*-EGDMA) recognitive gel is 2.2 times higher than the diffusion coefficient for poly(DEAEM-*co*-HEMA-*co*-PEG200DMA) recognitive gel ($(7.15 \pm 0.13) \times 10^{-9}$ and $(3.20 \pm 0.48) \times 10^{-9}$ cm^2/s, respectively). Considering the similarly sized template molecules, the EA9A-imprinted gels have a smaller average mesh size, 4.13 ± 0.2 Å, and the diclofenac sodium-imprinted gels have a larger average mesh size, 30.3 ± 1.7 Å. EA9A has a hydrodynamic radius in acetonitrile at 25°C of ~4.5 Å,[62] and diclofenac sodium has a hydrodynamic radius of ~4.3 Å[63,64] in water at 25°C. Because the mesh size/template hydrodynamic radius ratio is ~7.3 times higher for the poly(DEAEM-*co*-HEMA-*co*-PEG200DMA) recognitive gel, it would be expected to have faster template transport. The lower diffusion coefficient for the poly(DEAEM-*co*-HEMA-*co*-PEG200DMA) recognitive gel is a direct result of imprinting, and the template diffusion coefficients for imprinted polymers can be heavily influenced by template binding affinity. The template binding affinities calculated by Freundlich isotherm analysis for the poly(MAA-*co*-EGDMA) and the poly(DEAEM-*co*-HEMA-*co*-PEG200DMA) recognitive gels were 2.45 ± 0.13 and 15.05 ± 0.82 mM^{-1}, respectively. Although mesh size and template molecular size are important factors in diffusional transport, there was a relatively large increase in template binding affinity, which results in a significant increase in the template–polymer chain interaction. The increase in binding affinity influences template release through stronger intrinsic macromolecular recognition. Diclofenac sodium would diffuse through the gel binding and rebinding to macromolecular memory sites with strong ionic noncovalent bonding on its way through the network, whereas EA9A would have to diffuse through the network binding and rebinding to sites with relatively weak hydrogen bonding. The strength of the diclofenac sodium binding site is approximately six times stronger than the EA9A binding site. A stronger argument can be presented for the poly(DEAEM-*co*-HEMA-*co*-PEG200DMA) recognitive gels prepared via LCP because there is a 6.6-fold increase in template affinity with a 4.9-fold decrease in template transport with less difference in the polymer mesh size on the associated template release (i.e., the mesh size to template hydrodynamic radius ratios are 19.7 ± 2.1 for the poly(DEAEM-*co*-HEMA-*co*-PEG200DMA) gel and 4.13 ± 0.30 for the poly(MAA-*co*-EGDMA) gel prepared by LCP). Therefore, it is clear that imprinting plays an important role in the transport of the template from the network.

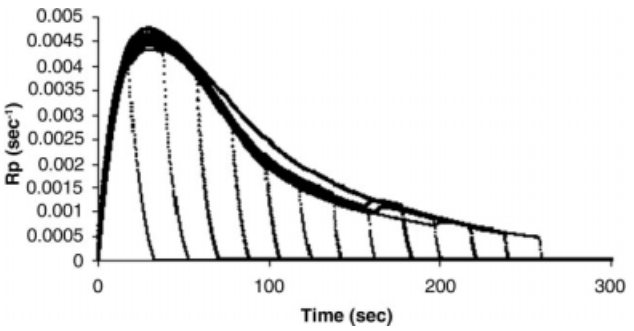

Figure 6. Poly(MAA-*co*-EGDMA) dark reaction kinetic analysis.

Thirteen reactions demonstrate the dark reaction analysis for the determination of propagation and termination kinetic constants. This graph represents the rate of polymerization of poly(MAA-*co*-EGDMA) control gel vs. time.

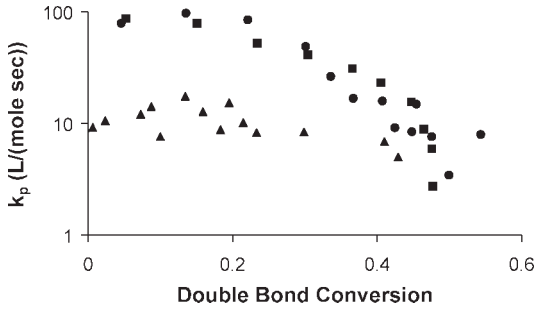

Figure 7. Propagation constants from Poly(MAA-*co*-EGDMA) gel kinetic analysis.

The propagation constant for the poly(MAA-*co*-EGDMA) recognitive gel (■)and control gel (●) had statistically similar trends with double bond conversion. Chemically controlled propagation mechanism occurs until 0.23 fractional double bond conversion. Higher conversions have a decrease in propagation indicating diffusion-controlled propagation. The "living/controlled" recognitive gel (▲) shows a more constant rate of propagation until a fractional double bond conversion of 0.40 indicating a longer chemical-controlled propagation mechanism.

Reaction kinetics

The kinetic parameters of the poly(MAA-*co*-EGDMA) gel reaction were analyzed to determine what changes the "living" polymerization technique had upon the kinetic constants of propagation and termination. Thirteen dark reactions for the kinetic analysis for poly(MAA-*co*-EGDMA)

control gel are shown in Figure 6. The propagation constant k_p, termination constant k_t, and k_t/k_p vs. double bond conversion for recognitive and control gels are shown in Figures 7–9, respectively.

The propagation constant vs. conversion (Figure 7) for the poly(MAA-*co*-EGDMA) recognitive and control gel follow typical experimental values found in the literature.[54,55,65] The propagation constant remains relatively constant where the chemical reaction is controlling the propagation mechanism for the gels (less than 0.23 fractional double bond conversion). At higher conversions, the propagation constant for the recognitive and control gel starts to decrease indicating that the propagation is being controlled by the diffusion-controlled mechanism. The diffusion-controlled propagation mechanism is where the controlling factor is the radical diffusing through the network to react with double bonds, thus propagating chains.[66]

For the ''living/controlled'' recognitive gel, propagation remains relatively constant until the fractional double bond conversion reaches 0.3 and 0.4. This indicates that the addition of iniferter increases the amount of network formed during the chemical reaction-controlled propagation mechanism. After a fractional double bond conversion of 0.4, the propagation constant decreases indicating the diffusion-controlled propagation mechanism.

The termination constants for the poly(MAA-*co*-EGDMA) control, recognitive gels, and gels prepared via ''living/controlled'' techniques have similar trends (Figure 8). The termination constant, k_t, vs. conversion has a relatively constant range with a decrease of termination constant at higher conversions. Typically, the termination constant has three regions. The regions are represented by an increase, a plateau, and a decrease in termination constant. These regions represent termination through segmental diffusion, limitation of segmental diffusion and the increasing dominance of reaction diffusion, and diffusion-controlled termination dependent upon propagating events, respectively. The segmental diffusion for the poly(MAA-*co*-EGDMA) networks is not evident in the data. Crosslinking reactions have a much earlier onset of gelation as early as 5% conversion.[55] The reactions presented in Figure 8 have the first data point at or above 5% conversion. Evident with the poly(MAA-*co*-EGDMA) gels is the plateau region from a fractional double bond conversion of (0.05–0.42). Segmental diffusion is limited and the reaction diffusion becomes increasingly dominant during this section of the polymerization. After a fractional double bond conversion of 0.42, the termination constant decreases which is consistent with literature. The decrease in the termination constant at higher double bond conversions is due to a decrease in propagation events and monomer-controlled diffusion. The ratio of k_t/k_p is shown in Figure 9.

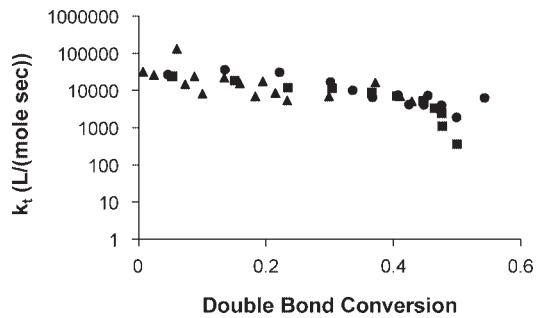

Figure 8. Termination constants from poly(MAA-*co*-EGDMA) gel kinetic analysis.

The termination constant for the poly(MAA-*co*-EGDMA) recognitive gel (■), control gel (●), and ''living/controlled'' recognitive gel (▲) shows statistically similar trends.

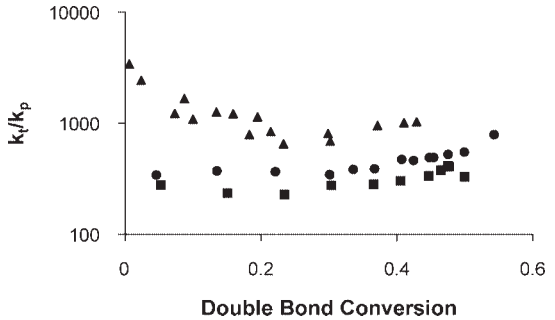

Figure 9. Ratio of k_t/k_p from poly(MAA-*co*-EGDMA) gel kinetic analysis.

Recognitive gel (■), control gel (●), and ''living/controlled'' recognitive gel (▲). It is important to note that both the propagation and termination constant trends matched literature trends for the copolymer networks.

The results from the kinetic analysis for the poly(MAA-*co*-EGDMA)-imprinted gels indicate that LCP specifically increases the chemical-controlled propagation mechanism. The increase in the chemical-controlled propagation mechanism in combination with binding capacity increases for these gels indicates that effective binding sites are formed during the chemical-controlled segment of the polymerization.

LCPs have reversible termination that increases the chemical-controlled propagation mechanism during which the growing polymer chains are less hindered by diffusional and structural limitations of the forming polymer network. By increasing the duration of the chemical-controlled propagation mechanism through ''living'' polymerization techniques, the growing polymer chains (i.e., including growing polymer chains forming macromolecular memory) would have more time during the reaction to move to the lowest energy conformation. It is hypothesized that these types of limitations lead to frustrations within the gel, which prevent growing polymer chains from forming macromolecular memory.

Conclusions

This work confirms the hypothesis that molecular imprinting via LCP techniques substantially increased the template loading/capacity and delayed the template release compared with conventional free-radical polymerization methodologies. This is the first proof and discussion of this phenomenon within weakly crosslinked structures. Also, this article presents anti-inflammatory imprinted hydrogels for the first time, which could be used to develop anti-inflammatory therapeutic contact lenses.

The poly(DEAEM-*co*-HEMA-*co*-PEG200DMA)-imprinted gel had a 140% increase in template loading over that of the control network, with loading capacities of $(0.96 \pm 0.12$ and $2.30 \pm 0.20) \times 10^{-2}$ mmol/g. The imprinted gel prepared

via LCP had a 54% increase in template loading capacity $(3.54 \pm 0.16) \times 10^{-2}$ mmol/g) compared with the imprinted gel and a 269% increase compared with the control gel. Both imprinted gels had ~1.5 times higher template binding affinity than the control gel, which had a template binding affinity of 9.91 ± 0.49 mM^{-1}. Similar trends and numerical values in capacity and percent increase in capacity were achieved with the poly(MAA-*co*-EGDMA) system. Template diffusion coefficients for the control gel, imprinted gel, and the imprinted gel prepared via LCP were $6.37 \pm 1.02 \times 10^{-9}$ cm^2/s, $3.20 \pm 0.48 \times 10^{-9}$ cm^2/s, and $1.49 \pm 0.33 \times 10^{-9}$ cm^2/s, respectively. The imprinted gel and imprinted gel prepared via LCP release profiles were less Fickian and moved closer toward zero-order release.

Reaction analysis confirmed that these results were not due to differences in double bond monomer conversion or incorporation of different amounts of functional monomer within the networks. Analysis of the reaction kinetics indicated that LCP with reversible termination events specifically increases the chemically controlled chain propagation mechanism, and that binding sites are formed during this phase of the polymerization. This allowed more effective macromolecular memory because of additional time to reach a lower energy conformation. Comparing both systems, it was clear that imprinting plays an important role in the delay of template transport from the network. Comparing poly (DEAEM-*co*-HEMA-*co*-PEG200DMA)- and poly(MAA-*co*-EGDMA)- imprinted gels prepared via LCP, there was a 6.6-fold increase in template affinity with a 4.9-fold decrease in template transport for the poly(DEAEM-*co*-HEMA-*co*-PEG200DMA)-imprinted gel with a five times higher mesh size/template hydrodynamic ratio. Therefore, imprinting LCP techniques have tremendous potential for the design, engineering, and enhancement of weakly crosslinked networks as advanced drug delivery carriers.

Acknowledgments

The authors acknowledge funding from NSF CBET (NSF-CBET-0730903, grant G00003191), GAANN (GAANN grant P200A060184, ADV is a U.S. Department of Education GAANN fellow). They thank Dr. Maria Auad of Auburn University for the use of DMA.

Literature Cited

1. Peppas NA, Bar-Howell BD. *Hydrogels in Medicine and Phamacy*, Vol. 1. Boca Raton: CRC Press, 1987.
2. Venkatesh S, Saha J, Pass S, Byrne ME. Transport and structural analysis of molecular imprinted hydrogels for controlled drug delivery. *Eur J Pharm Biopharm*. 2008;69:852–860.
3. Venkatesh S, Sizemore SP, Byrne ME. Biomimetic hydrogels for enhanced loading and extended release of ocular therapeutics. *Biomaterials*. 2007;28:717–724.
4. Ali M, Horikawa S, Venkatesh S, Saha J, Hong JW, Byrne ME. Zero-order therapeutic release from imprinted hydrogel contact lenses within in vitro physiological ocular tear flow. *J Controlled Release*. 2007;124:154–162.
5. Alvarez-Lorenzo C, Hiratani H, Gomez-Amoza JL, Martinez-Pacheco R, Souto C, Concheiro A. Soft contact lenses capable of sustained delivery of timolol. *J Pharm Sci*. 2002;91:2182–2192.
6. Alvarez-Lorenzo C, Yanez F, Barreiro-Iglesias R, Concheiro A. Imprinted soft contact lenses as norfloxacin delivery systems. *J Controlled Release*. 2006;113:236–244.
7. Hiratani H, Fujiwara A, Tamiya Y, Mizutani Y, Alvarez-Lorenzo C. Ocular release of timolol from molecularly imprinted soft contact lenses. *Biomaterials*. 2005;26:1293–1298.
8. Ali M, Byrne ME. Controlled release of high molecular weight hyaluronic acid from molecularly imprinted hydrogel contact lenses. *Pharm Res*. 2009;26:714–726.
9. Byrne ME, Salian V. Molecular imprinting within hydrogels. II. Progress and analysis of the field. *Int J Pharm*. 2008;364:188–212.
10. Otsu T, Yoshida M. Role of initiator-transfer agent-terminator (iniferter) in radical polymerizations: polymer design by organic disulfides as iniferters. *Makromol Chem Rapid Commun*. 1982; 3:127–132.
11. Matyjaszewski K. A commentary on "role of initiator-transfer agent-terminator (Iniferter) in radical polymerizations: polymer design by organic disulfides as iniferters" by T. Otsu, M. Yoshida (Macromol. Rapid Commun. 1982,3, 127–132). *Macromol Rapid Commun*. 2005;26:135–142.
12. Haddleton DM, Kukulj D, Duncalf DJ, Heming AM, Shooter AJ. Low-temperature living "radical" polymerization (atom transfer polymerization) of methyl methacrylate mediated by copper(I) N-alkyl-2-pyridylmethanimine complexes. *Macromolecules*. 1998;31:5201–5205.
13. Endo K, Murata K, Otsu T. Living radical polymerization of styrene with tetramethylene disulfide. *Macromolecules*. 1992;25: 5554–5556.
14. Ward JH, Peppas NA. Kinetic gelation modeling of controlled radical polymerizations. *Macromolecules*. 2000;33:5137–5142.
15. Matyjaszewski K, Jo SM, Paik HJ, Gaynor SG. Synthesis of well-defined polyacrylonitrile by atom transfer radical polymerization. *Macromolecules*. 1997;30:6398–6400.
16. High K, Meng Y, Washabaugh MW, Zhao Q. Determination of picomolar equilibrium dissociation constants in solution by enzyme-linked immunosorbent assay with fluorescence detection. *Anal Biochem*. 2005;347:159–161.
17. Qin DQ, Qin SH, Qiu KY. A reverse ATRP process with a hexasubstituted ethane thermal iniferter diethyl 2,3-dicyano-2,3-di(p-tolyl)-succinate as the initiator. *Macromolecules*. 2000;33:6987–6992.
18. Qin L, He X-W, Li W-Y, Zhang Y-K. Molecularly imprinted polymer prepared with bonded β-cyclodextrin and acrylamide on functionalized silica gel for selective recognition of tryptophan in aqueous media. *J Chromatogr A*. 2008;1187:94–102.
19. Baek SH, Kim BS, Kim BK. Hydrogels based on polyurethane-polyacrylic acid multiblock copolymers via macroiniferter technique. *Prog Org Coat*. 2004;49:353–357.
20. Chen H, Peng C, Ye Z, Liu H, Hu Y, Jiang J. Recognition of multiblock copolymers on nanopatterned surfaces: insight from molecular simulations. *Langmuir*. 2007;23:2430–2436.
21. Cheng Z, Zhu X, Fu GD, Kang ET, Neoh KG. Dual-brush-type amphiphilic triblock copolymer with intact epoxide functional groups from consecutive RAFT polymerizations and ATRP. *Macromolecules*. 2005;38:7187–7192.
22. Gabashvili A, Medina DD, Gedanken A, Mastai Y. Templating mesoporous silica with chiral block copolymers and its application for enantioselective separation. *J Phys Chem B*. 2007;111:11105–11110.
23. Kwon IK, Matsuda T. Photo-iniferter-based thermoresponsive block copolymers composed of poly(ethylene glycol) and poly(N-isopropylacrylamide) and chondrocyte immobilization. *Biomaterials*. 2006;27:986–995.
24. Qin Y, Sukul V, Pagakos D, Cui C, Jakle F. Preparation of organoboron block copolymers via ATRP of silicon and boron-functionalized monomers. *Macromolecules*. 2005;38:8987–8990.
25. de Boer B, Simon HK, Werts MPL, van der Vegte EW, Hadziioannou G. "Living" free radical photopolymerization initiated from surface-grafted iniferter monolayers. *Macromolecules*. 2000; 33:349–356.
26. Francis R, Ajayaghosh A. Minimization of homopolymer formation and control of dispersity in free radical induced graft polymerization using xanthate derived macro-photoinitiators. *Macromolecules*. 2000;33:4699–4704.
27. Lee HJ, Nakayama Y, Matsuda T. Spatio-resolved, macromolecular architectural surface: highly branched graft polymer via photochemically driven quasiliving polymerization technique. *Macromolecules*. 1999;32:6989–6995.
28. Liu P, Liu Y, Su Z. Modification of poly(hydroethyl acrylate)-grafted cross-linked poly(vinyl chloride) particles via surface-initiated atom-transfer radical polymerization (SI-ATRP). Competitive

adsorption of some heavy metal ions on modified polymers. *Ind Eng Chem Res*. 2006;45:2255–2260.
29. Matsuda T, Ohya S. Photoiniferter-based thermoresponsive graft architecture with albumin covalently fixed at growing graft chain end. *Langmuir*. 2005;21:9660–9665.
30. Nakayama Y, Sudo M, Uchida K, Matsuda T. Spatio-resolved hyperbranched graft polymerized surfaces by iniferter-based photograft copolymerization. *Langmuir*. 2002;18:2601–2606.
31. Hutchison JB, Lindquist AS, Anseth KS. Experimental characterization of structural features during radical chain homopolymerization of multifunctional monomers prior to macroscopic gelation. *Macromolecules*. 2004;37:3823–3831.
32. Kannurpatti AR, Anderson KJ, Anseth JW, Bowman CN. Use of "living" radical polymerizations to study the structural evolution and properties of highly crosslinked polymer networks. *J Polym Sci Part B: Polym Phys*. 1997;35:2297–2307.
33. Smith D, Pentzer EB, Nguyen ST. Bioactive and therapeutic ROMP polymers. *Polym Rev*. 2007;47:419–459.
34. Ding S, Xing Y, Radosz M, Shen Y. Magnetic nanoparticle supported catalyst for atom transfer radical polymerization. *Macromolecules*. 2006;39:6399–6405.
35. Yang J, Ding S, Radosz M, Shen Y. Reversible catalyst supporting via hydrogen-bonding-mediated self-assembly for atom transfer radical polymerization of MMA. *Macromolecules*. 2004;37:1728–1734.
36. Chen XP, Qiu KY. Synthesis of well-defined poly(methyl methacrylate) by radical polymerization with a new initiation system TPED/FeCl3/PPh3. *Macromolecules*. 1999;32:8711–8715.
37. Sugihara Y, Kagawa y, Yamago S, Okubo M. Organotellurium-mediated living radical polymerization in miniemulsion. *Macromolecules*. 2007;40:9208–9211.
38. Hawker CJ, Bosman AW, Harth E. New polymer synthesis by nitroxide mediated living radical polymerizations. *Chem Rev*. 2001;101:3661–3688.
39. Kannurpatti AR, Lu S, Bunker GM, Bowman CN. Kinetic and mechanistic studies of iniferter photopolymerizations. *Macromolecules*. 1996;29:7310–7315.
40. Vaughan AD, Byrne ME. Optimizing recognition characteristics of biomimetic polymer gels via polymerization reaction and crosslinking density analysis. *ACS PMSE Preprints*. 2006;94:762–763.
41. Boonpangrak S, Whitcombe MJ, Prachayasittikul V, Mosbach K, Yei L. Preparation of molecularly imprinted polymers using nitroxide-mediated living radical polymerization. *Biosens Bioelectron*. 2006;22:349–354.
42. Vaughan AD, Sizemore SP, Byrne ME. Enhancing molecularly imprinted polymer binding properties via controlled/living radical polymerization and reaction analysis. *Polymer*. 2007;48:74–81.
43. Rueckert B, Hall AJ, Sellergren B. Molecularly imprinted composite materials via iniferter-modified supports. *J Mater Chem*. 2002; 12:2275–2280.
44. Wei X, Li X, Husson SM. Surface molecular imprinting by atom transfer radical polyemrization. *Biomacromolecules*. 2005; 6:1113–1121.
45. Hägerström H, Paulsson M, Edsman K. Evaluation of mucoadhesion for two polyelectrolyte gels in simulated physiological conditions using a rheological method. *Eur J Pharm Sci*. 2000; 9:301–309.
46. Crank J. *The Mathematics of Diffusion*. New York: Oxford University Press, 1975.
47. Sperling LH. *Introduction to Physical Polymer Science*, 4th ed. Hoboken: Wiley, 2005.
48. Flory PJ. *Principles of Polymer Chemistry*, 1st ed. Ithaca: Cornell University Press, 1953:663.
49. Brazel CS, Peppas NA. Synthesis and characterization of thermo- and chemomechanically responsive poly(N-isopropylacrylamide-co-methacrylic acid) hydrogels. *Macromolecules*. 1995;28:8016–8020.
50. Kavimandan NJ, Losi E, Peppas NA. Novel delivery system based on complexation hydrogels as delivery vehicles for insulin-transferrin conjugates. *Biomaterials*. 2006;27:3846–3854.
51. Berger J, Reist M, Mayer JM, Felt O, Peppas NA, Gurny R. Structure and interactions in covalently and ionically crosslinked chitosan hydrogels for biomedical applications. *Eur J Pharm Biopharm*. 2004;57:19–34.
52. Hariharan D, Peppas NA. Characterization, dynamic swelling behaviour and solute transport in cationic networks with applications to the development of swelling-controlled release systems. *Polymer*. 1996;37:149–161.
53. Lowman AM, Dziubla TD, Bures P, Peppas NA. *Structural and dynamic response of neutral and intelligent networks in biomedical environments*. In: NA Peppas and MV Sefton, Eds. *Molecular and Cellular Foundations of Biomaterials*, Vol. 29. New York: Academic Press, 2004:75–130.
54. Anseth KS, Kline LM, Walker TA, Anderson KJ, Bowman CN. Reaction kinetics and volume relaxation during polymerizations of multiethylene glycol dimethacrylates. *Macromolecules*. 1995;28: 2491–2499.
55. Anseth KS, Wang CM, Bowman CN. Reaction behaviour and kinetic constants for photopolymerizations of multi(meth)acrylate monomers. *Polymer*. 1994;35:3243–3250.
56. Odian G. *Principles of Polymerization*, 2nd ed. New York: Wiley, 1981.
57. Smith DA, Wallwork ML, Zhang J, Kirkham J, Robinson C, Marsh A, Wong M. The effect of electrolyte concentration on the chemical force titration behavior of ω-functionalized SAMs: evidence for the formation of strong ionic hydrogen bonds. *J Phys Chem B*. 2000;104:8862–8870.
58. Srinivasan R, Feenstra JS, Park ST, Xu S, Zewail AH. Direct determination of hydrogen-bonded structures in resonant and tautomeric reactions using ultrafast electron diffraction. *J Am Chem Soc*. 2004;126:2266–2267.
59. Noss KR, Vaughan AD, Byrne ME. Tailored binding and transport parameters of molecularly imprinted films via macromolecular structure: the rational design of recognitive polymers. *J Appl Polym Sci*. 2008;107:3435–3441.
60. Bell CL, Peppas NA. Water, solute and protein diffusion in physiologically responsive hydrogels of poly(methacrylic acid-*g*-ethylene glycol). *Biomaterials*. 1996;17:1203–1218.
61. Spizzirri UG, Peppas NA. Structural analysis and diffusional behavior of molecularly imprinted polymer networks for cholesterol recognition. *Chem Mater*. 2005;17:6719–6727.
62. Vega J, Michaelian K, Garzón IL, Beltrán MR, Hernández L. Isomers of adenine. *J Mol Struct: THEOCHEM*. 1999;493:275–285.
63. Maitani Y, Kugo M, Nakagaki M, Nagai T. Ionic size and behavior of diclofenac salts in water and ethanol/water mixtures by conductivity at 25°C. *J Pharm Sci*. 1993;82:1245–1249.
64. Mandal R, Gangopadhyay J, Lahiri SC. Studies on hydrophobic interaction from the conductometric studies of medicinal compounds (as salts). *Z Phys Chem*. 2005;219:795–805.
65. Khudyakov IV, Legg JC, Purvis MB, Overton BJ. Kinetics of photopolymerization of acrylates with functionality of 1–6. *Ind Eng Chem Res*. 1999;38:3353–3359.
66. Sigwalt P, Moreau M. Carbocationic polymerization: mechanisms and kinetics of propagation reactions. *Prog Polym Sci*. 2006;31:44–120.

Manuscript received Dec. 23, 2008, and revision received Apr. 13, 2009.